CHIN. PHYS. LETT. Vol. 35, No. 4 (2018) 043203

Experimental Determination of the Landé g-Factors for $5s^2\,{}^1S$ and $5s5p\,{}^3P$ States of the ^{87}Sr Atom *

Ben-quan Lu(卢本全)[1,2,3], Yebing Wang(王叶兵)[1,2], Yang Guo(郭阳)[1,2], Qinfang Xu(徐琴芳)[1], Mojuan Yin(尹默娟)[1], Jiguang Li(李冀光)[3], Hong Chang(常宏)[1,2]**

[1]*National Time Service Center, Xi'an 710000*
[2]*University of Chinese Academy of Sciences, Beijing 100049*
[3]*Institute of Applied Physics and Computational Mathematics, Beijing 100088*

(Received 23 January 2018)

We present an experimental determination on the Landé g-factors for the $5s^2\,{}^1S_0$ and $5s5p\,{}^3P_0$ states in ultra-cold atomic systems, which is important for evaluating the Zeeman shift of the clock transition in the ^{87}Sr optical lattice clock. The Zeeman shift of the $5s5p\,{}^3P_0$–$5s^2\,{}^1S_0$ forbidden transition is measured with the π-polarized and $\sigma^{\pm}$-polarized interrogations at different magnetic field strengths. Moreover, in the g-factor measurement with the $\sigma^{\pm}$-transition spectra, it is unnecessary to calibrate the external magnetic field. By this means, the ground state $5s^2\,{}^1S_0$ g-factor for the ^{87}Sr atom is $-1.306(52)\times10^{-4}$, which is the first experimental determination to the best of our knowledge, and the result matches very well with the theoretical estimation. The differential g-factor δg between the $5s5p\,{}^3P_0$ state and the $5s^2\,{}^1S_0$ state of the ^{87}Sr atoms is measured in the experiment as well, which are $-7.67(36)\times10^{-5}$ with π-transition spectra and $-7.72(43)\times10^{-5}$ with $\sigma^{\pm}$-transition spectra, in good agreement with the previous report [Phys. Rev. A 76 (2007) 022510]. This work can also be used for determining the differential g-factor of the clock states for the optical clocks based on other atoms.

PACS: 32.60.+i, 37.10.Jk, 32.30.−r DOI: 10.1088/0256-307X/35/4/043203

In the past few years, optical atomic clocks[1–4] have been widely and deeply studied as they have higher accuracy and stability compared with microwave atomic clocks.[5] Moreover, the optical clocks have shown potential applications in precise measurement for tests of fundamental physical constants,[6–9] navigation and timekeeping,[10,11] definition of the second[12] and study of many-body quantum systems.[13,14] Recently, the optical lattice clock based on ^{87}Sr atoms is reported to be one of the most accurate clocks, and its uncertainty and stability achieved 10^{-18}.[15,16] To improve the accuracy of the optical clock, it is necessary to determine the atomic parameters more accurately. The Landé g-factors of the clock states are one of the important atomic parameters as the g-factors reflect the sensitivity of the atomic state to the external magnetic field. According to the g-factors of the clock states, the Zeeman shift of the clock transitions can be estimated for the optical clocks.

As is known, in diamagnetic molecules and atoms, the g-factors of the electric states are easily affected by the chemical shift.[17] For the alkaline-earth-like atoms and ions, the g-factors of the $^1S_0$ and $^3P_0$ states are not only affected by the chemical shift but also affected by the state mixing induced by the hyperfine coupling. The g-factors of these atoms and ions have been determined for estimating the Zeeman shift in the optical clocks based on the alkaline-earth-like atoms and ions, such as ^{199,201}Hg,[17,18] ^{199}Hg$^+$,[19] ^{41}Ca$^+$,[20] ^{171}Yb$^+$,[21] ^{171}Yb,[22] ^{87}Sr[23] and ^{27}Al$^+$.[24] The g-factor of the ^{87}Sr atom in the ground state is $g(5s^2\,{}^1S_0)=(1-\sigma_{\rm d})g_{\rm I}$, where $\sigma_{\rm d}$ is the diamagnetic correction (one of the chemical shift corrections), and $g_{\rm I}$ is the g-factor of the bare nucleus. The g-factor of the ground state has been theoretically estimated.[23] However, there is no report on the experimental determination of the $g(5s^2\,{}^1S_0)$ of the ^{87}Sr atom yet. As the difference between the diamagnetic correction $\sigma_{\rm d}$ of the ground state and the $5s5p\,{}^3P_0$ state is negligibly small, the g-factor of the $^3P_0$ state is $g(5s5p\,{}^3P_0)=g(5s^2\,{}^1S_0)+\delta g$, where δg describes the differential g-factor of the clock states of the ^{87}Sr atom. The experimental and the theoretical determinations of the differential g-factor δg have been demonstrated.[23] Boyd *et al.*[23] calculated the values of δg using the Breit–Will (BW) and the modified BW (MBW) theories and measured it with the $\sigma^{\pm}$-transition spectra. The deviation between the calculated result by the MBW theory and the experimental results is about 8%.

In this Letter, we experimentally determine the g-factor of the ground state $g(5s^2\,{}^1S_0)$ and measured the differential g-factor between the $5s^2\,{}^1S_0$ state and the $5s5p\,{}^3P_0$ state in the ultra-cold ^{87}Sr atomic system. The g-factors were measured according to the Zeeman shift of the $5s5p\,{}^3P_0$–$5s^2\,{}^1S_0$ forbidden transition, which was interrogated by π-polarization and $\sigma^{\pm}$-polarization at different magnetic field strengths. It is the first experimental determination of the ground

*Supported by the National Natural Science Foundation of China under Grant Nos 61127901, 11404025 and 91536106, the Strategic Priority Research Program of the Chinese Academy of Sciences under Grant No XDB21030700, the Key Research Project of Frontier Science of Chinese Academy of Sciences under Grant No QYZDB-SSW-JSC004, and the China Postdoctoral Science Foundation under Grant No 2014M560061.

**Corresponding author. Email: changhong@ntsc.ac.cn

© 2018 Chinese Physical Society and IOP Publishing Ltd

state g-factor for the ^{87}Sr atom, and the result agrees with the theoretical estimation. Moreover, in the measurement with the $\sigma^{\pm}$-transition spectra, it is unnecessary to calibrate the external magnetic field. The differential g-factor measured in our experiment shows very good consistence with the previous report.[23] The experimental results of the differential g-factor δg can be used as a reference for the theoretical estimation using the hyperfine induced state mixing theory. The results of the present work suggest that the hyperfine induced state mixing plays an important role in the accurate determination of the atomic parameters.

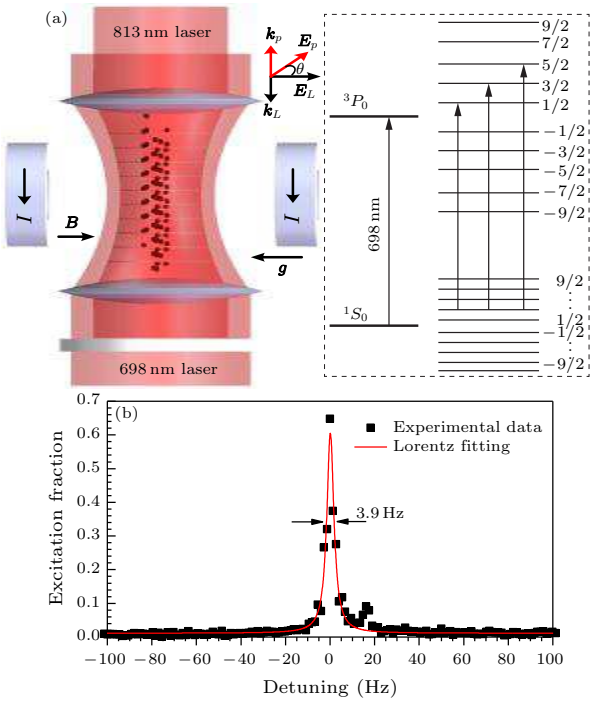

Fig. 1. (a) Schematic of the experimental apparatus used for measuring the clock transition and the energy level of the $^1S_0$ and $^3P_0$ clock states of the ^{87}Sr atom in the circumstance of the magnetic field $\boldsymbol{B}$. The large nuclear spin results in 28 transitions. The labels π, σ^+ and σ^- represent the transitions which change the magnetic quantum number m_F by 0, -1 and $+1$. Here $\boldsymbol{g}$ represents the acceleration of gravity. (b) Spectrum of the clock transition at zero magnetic field. The linear polarizations of the probe laser and the lattice laser have the same direction ($\theta = 0°$). A Lorentzian fitting to the experimental data yields a line width of 3.9 Hz.

According to the hyperfine interaction, the fine structure energy level is split (hyperfine splitting) in the ^{87}Sr atom with the nuclear spin $I = 9/2$. In a weak external magnetic field, the hyperfine structure energy level will be shifted. In the optical lattice, the Doppler shift and the recoil energy shift of the atomic clock transition can be canceled, which leads to a more precise measurement of the Zeeman shift. In the ^{87}Sr optical lattice clock, by scanning the frequency of the 698-nm clock laser, a clock transition spectrum with several peaks can be achieved. These peaks are corresponding to the transitions between the ground and the excited sublevels. By accurately measuring the frequency interval between the neighboring two peaks, the Landé g-factor $g(5s^2\,{}^1S_0)$ and the differential g-factor δg can be obtained. To determine g-factors, it is necessary to carefully calibrate the external magnetic field and accurately control the frequency of the probe laser. In our experiment, the π-transition spectra and the $\sigma^{\pm}$-transition spectra were used to determine the g-factors. With π-transition spectra, we accurately calibrated the external magnetic field and precisely measured the relative Zeeman shift. Since the frequency of the probe laser was locked to a stable ultra-low expansion cavity, the measured accuracy of the Zeeman shift can reach the Hz level. Then, according to the $\sigma^{\pm}$-transition spectra, the values of $g(5s^2\,{}^1S_0)$ and δg can be determined without the calibration of the external magnetic field.

The schematic of the experimental apparatus is shown in Fig. 1(a). After two-stage cooling, the ultracold ^{87}Sr atoms were loaded into the one-dimensional lattice. The preparation of cold atoms was described in detail in Ref. [25]. About 10^4 atoms were trapped in the optical lattice at a temperature of 3 μK. The potential of the lattice is $U_{\rm T} = 35E_{\rm R}$, where $E_{\rm R}$ is the recoil energy. The optical lattice was operated at the 'magic wavelength' of $\lambda_{\rm L} = 813.4280(5)$ nm.[4,26–28] The wave vector of the 813-nm laser $\boldsymbol{k}_{\rm L}$ was perpendicular to the gravity. The probe laser at 698 nm was locked to a stable ultra-low expansion cavity, which yielded a line width of about 1 Hz. The frequency of the probe laser was modulated by an acousto-optical modulator (AOM). The wave vector of the 698-nm laser ($\boldsymbol{k}_{\rm p}$) was opposite to that of the 813-nm laser $\boldsymbol{k}_{\rm L}$, and the linear polarization angle of the probe laser was set at θ relative to the polarization of the lattice laser, as shown in Fig. 1(a). The beam waist ($1/e^2$ radius of intensity) of the 698-nm laser was approximately three times larger than that of the 813-nm laser. In the vertical direction, a static magnetic field was produced by a pair of Helmholtz coils, and its direction was parallel to the linear polarization of the 813-nm laser. Two other coil pairs were used to offset the magnetic field in the horizontal direction. As the $^3P_0$ state is a metastable state, we used the shelved detection method[29] to measure the excitation fraction. The 461-nm laser, which was operated at the $5s^2\,{}^1S_0$–$5s5p\,{}^1P_1$ transition wavelength, was used to measure the number of the atoms. As the 461-nm laser pulse would destruct the atomic trapping, the atoms should be re-trapped after each step of clock probing. The energy levels of the $^1S_0$ and $^3P_0$ clock states in the presence of the magnetic field are also shown in Fig. 1(a). Since the corresponding g-factors are different, energy shifts for the ground and the excited states are different in Fig. 1(a). According to the energy levels, there are 28 transitions, labeled as π, σ^+ and σ^- between the ground Zeeman states and the excited Zeeman states. Figure 1(b) shows the narrowest spectrum of the clock transition with degenerate sublevels obtained in our present apparatus. The probe time of the 698-nm laser was 300 ms. A Lorentzian

fitting to the experimental data yields a line width of 3.9 Hz, which corresponds to a Fourier-limited line width of 3 Hz.

In the experiment, we used a liquid crystal waveplate to control the polarization of the 698-nm laser precisely. When the polarization direction was along the direction of the magnetic field ($\theta = 0°$), the π-transition spectrum was obtained. When the polarization direction was perpendicular to the direction of the magnetic field ($\theta = 90°$), the $\sigma^{\pm}$-transition was obtained. The spectra of the π-transition and the $\sigma^{\pm}$-transition are shown in Figs. 2(a) and 2(b), respectively. The experimental data are shown in black with the Lorentzian fitting in red. The peaks in the spectra are labeled according to the ground sublevel state quantum number m_F and the excitation polarization. The relative intensity for the different ground sublevel states is mainly influenced by the Clebsch–Gordan coefficients.

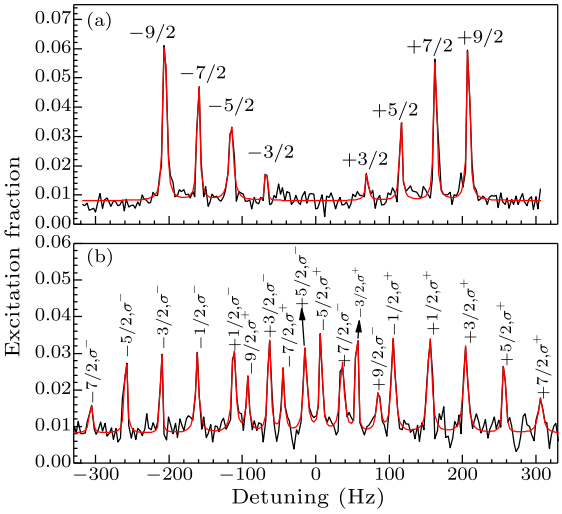

Fig. 2. (a) The π-transition spectrum with a magnetic field strength $B = 0.434$ G, and (b) the $\sigma^{\pm}$-transition spectrum with a magnetic field strength $B = 0.463$ G. The labels presented in the figures are the transitions from the ground sublevel state, as well as the excitation polarization.

In the presence of a magnetic field, the frequency of the π-transition ($\Delta m_F = 0$) from ground sublevel state m_F reads

$$\begin{aligned} \upsilon_{\pi_{m_F}} =& \upsilon_{\rm c} - (\Delta\kappa^{\rm S} - \Delta\kappa^{\rm T} F(F+1))\frac{U_{\rm T}}{E_{\rm R}} \\ & - (\Delta\kappa^{\rm V} m_F \xi\delta\phi + \Delta\kappa^{\rm T} 3m_F^2)\frac{U_{\rm T}}{E_{\rm R}} \\ & - \delta g m_F \mu_0 B, \end{aligned} \tag{1}$$

where $\upsilon_{\rm c}$ is the bare clock frequency, the second and third terms are the light shifts induced by the lattice potential, the last term is the Zeeman shift induced by the magnetic field, $\Delta\kappa$ is the shift coefficient due to the differential polarizabilities, $\Delta\kappa^{\rm S}$, $\Delta\kappa^{\rm V}$ and $\Delta\kappa^{\rm T}$ are the scalar, vector and tensor differential shift coefficients, respectively, ξ is the degree of elliptical polarization ($\xi = 0$ represents the linear polarization, $\xi = 1$ represents the circular polarization), and $\mu_0 = \frac{\mu_{\rm B}}{h}$ with $\mu_{\rm B}$ being the Bohr magneton and h being Planck's constant. The frequency difference between the neighboring peaks can be expressed as

$$\begin{aligned} f_{\pi,m_F} =& \upsilon_{\pi_{m_F}} - \upsilon_{\pi_{m_F-1}} \\ =& -\Delta\kappa^{\rm T} 3(2m_F - 1)\frac{U_{\rm T}}{E_{\rm R}} \\ & - \Delta\kappa^{\rm V}\xi\delta\phi\frac{U_{\rm T}}{E_{\rm R}} - \delta g\mu_0 B. \end{aligned} \tag{2}$$

If we neglect the small frequency shift induced by the lattice potential, Eq. (2) can be simplified to

$$f_{\pi,m_F} = \upsilon_{\pi_{m_F}} - \upsilon_{\pi_{m_F-1}} = -\delta g\mu_0 B. \tag{3}$$

Therefore, according to the π-transition spectrum, the differential g-factor δg can be expressed as

$$\delta g = -\frac{f_{\pi,m_F}}{\mu_0 B}. \tag{4}$$

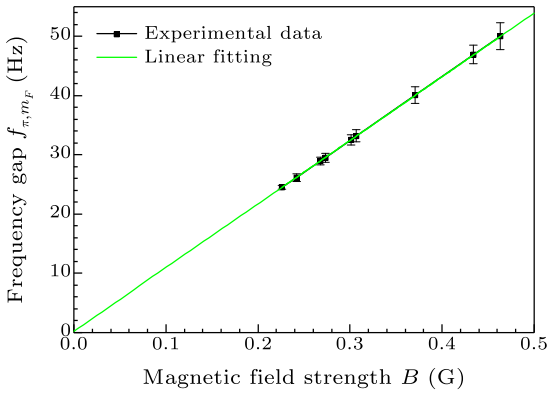

Fig. 3. The Zeeman shift as a function of the magnetic field strength in the π-transition spectra. The solid squares are the weighted average of several measurements with different magnetic field strengths, and the error bars are the standard deviation of our measurements. The green line is the linear fitting of the experimental data.

Determination of the Zeeman shift and the differential g-factor according to the π-transition is a traditional method. In this method, we carefully calibrated the external magnetic field and precisely controlled the frequency of the clock laser. The external magnetic field was calibrated by a magnetometer and the narrowest spectrum of the clock transition with degenerate sublevels in our current apparatus. The magnetic field strength fluctuation was controlled in the limit of 1 μT by accurately controlling the current of the Helmholtz coils. Simultaneously, it took about 300 s to obtain a clock transition spectrum. The linear frequency shift of the clock laser was less than 2 Hz in this time limit. In this experiment, we obtained 27 spectra of the π-transition in different magnetic field strengths. In each spectrum, there are eight observable lines. The $m_F = \pm\frac{1}{2}$ transitions are not observable as the corresponding transition rate is small. We used the Lorentzian function to fit the experimental results. According to Eqs. (3) and (4), we obtained the values of the differential g-factor

δg in different magnetic field strengths, as shown in Fig. 3. By linearly fitting the experimental data, we obtained $\delta g = -7.67(36) \times 10^{-5}$, where the number in the parentheses is the standard deviation of the measured value. The influences of the magnetic field strength fluctuation and the linear frequency shift of the clock laser were contained in the uncertainty.

Similarly, the frequencies of the $\sigma^{\pm}$-transitions ($\Delta m_F = 1$) from a ground sublevel state m_F can be given as

$$\begin{aligned} v_{\sigma^{\pm}_{m_F}} =& v_{\rm c} - (\Delta\kappa^{\rm S} - \Delta\kappa^{\rm T} F(F+1))\frac{U_{\rm T}}{E_{\rm R}} \\ & - ((\kappa_{\rm e}^{\rm V}(m_F \pm 1) - \kappa_{\rm g}^{\rm V} m_F)\xi\delta\phi)\frac{U_{\rm T}}{E_{\rm R}} \\ & - (\kappa_{\rm e}^{\rm T} 3(m_F \pm 1)^2 - \kappa_{\rm g}^{\rm V} 3m_F^2)\frac{U_{\rm T}}{E_{\rm R}} \\ & - (\pm g(5s^2\,{}^1S_0) + \delta g(m_F \pm 1))\mu_0 B, \end{aligned} \quad (5)$$

where $\kappa_{\rm g}$ and $\kappa_{\rm e}$ represent the shift coefficients of the ground and the excited states, individually.

For the neighboring lines of a specific transition (σ^+ or σ^- transition), the frequency gap is given as

$$\begin{aligned} f_{\sigma^{\pm},m_F} =& v_{\sigma^{\pm}_{m_F}} - v_{\sigma^{\pm}_{m_F-1}} \\ =& -\delta g\mu_0 B - (\kappa_{\rm e}^{\rm V} + \kappa_{\rm g}^{\rm V})\xi\delta\phi\frac{U_{\rm T}}{E_{\rm R}} \\ & - 3(2\kappa_{\rm e}^{\rm T} m_F(2m_F - 1 \pm 1) \\ & - \kappa_{\rm g}^{\rm V}(2m_F - 1))\frac{U_{\rm T}}{E_{\rm R}}. \end{aligned} \quad (6)$$

For the σ^+ and σ^- transitions of the same ground sublevel state, the frequency gap is given by

$$\begin{aligned} f_{d,m_F} =& v_{\sigma^{+}_{m_F}} - v_{\sigma^{-}_{m_F}} \\ =& -2\kappa_{\rm e}^{\rm V}\xi\delta\phi\frac{U_{\rm T}}{E_{\rm R}} - 12m_F\kappa_{\rm e}^{\rm T}\frac{U_{\rm T}}{E_{\rm R}} \\ & - 2(g(5s^2\,{}^1S_0) + \delta g)\mu_0 B. \end{aligned} \quad (7)$$

We can also neglect the small frequency shift induced by the lattice potential, then Eqs. (6) and (7) are simplified to

$$f_{\sigma^{\pm},m_F} = v_{\sigma^{\pm}_{m_F}} - v_{\sigma^{\pm}_{m_F-1}} = -\delta g\mu_0 B, \quad (8)$$

$$\begin{aligned} f_{d,m_F} =& v_{\sigma^{+}_{m_F}} - v_{\sigma^{-}_{m_F}} \\ =& -2(g(5s^2\,{}^1S_0) + \delta g)\mu_0 B. \end{aligned} \quad (9)$$

Therefore, according to the $\sigma^{\pm}$-transition spectrum, δg can be expressed as

$$\delta g = \frac{g(5s^2\,{}^1S_0)}{\frac{f_{d,m_F}}{2f_{\sigma^{\pm},m_F}} - 1} = \frac{(1-\sigma_{\rm d})g_{\rm I}}{\frac{f_{d,m_F}}{2f_{\sigma^{\pm},m_F}} - 1}, \quad (10)$$

where $\sigma_{\rm d} = 0.00345$,[30] $g_{\rm I} = \frac{\mu_{\rm I}}{I\mu_0}$, $\mu_{\rm I} = -1.0924(7)\mu_N$,[31] and μ_N is the nuclear magneton.

According to Eq. (10), the differential g-factor is directly related to the nuclear g-factor and the measured Zeeman shifts. It is unnecessary to calibrate the external magnetic field. In the experiment, we obtained 26 spectra of the $\sigma^{\pm}$-transition in different magnetic field strengths. There are 18 $\sigma^{\pm}$ transitions in each spectrum. By extracting the relative frequency gap of $f_{\sigma^{\pm},m_F}$ and f_{d,m_F}, we obtained 16 measured values of δg. According to the statistics on the values of δg from the 26 spectra, as shown in Fig. 4(a), finally we obtain $\delta g = -7.72(43) \times 10^{-5}$. The uncertainty is the standard deviation of the measured value. The linear laser drift is contained in the uncertainty. Moreover, the lattice potential effect on δg is less than 0.1%,[23] which is neglected in this measurement.

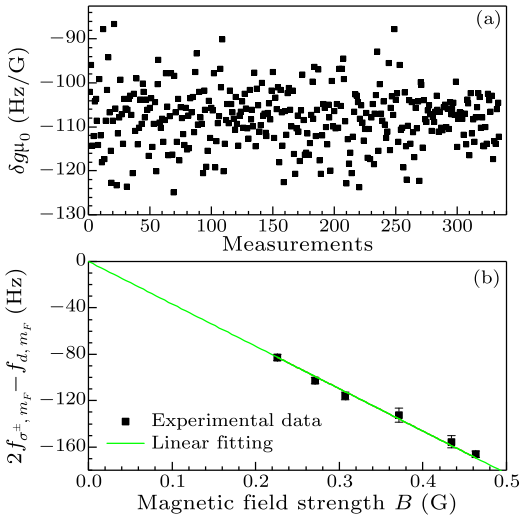

Fig. 4. (a) Measured values of $\delta g\mu_0$ (Hz·G^{-1}) according to the $\sigma^{\pm}$-transition spectrums. (b) Measured values of $2f_{\sigma^{\pm},m_F} - f_{d,m_F}$ (Hz) as a function of the magnetic field strength.

For the g-factor of the ground state $g(5s^2\,{}^1S_0)$, according to Eqs. (8) and (9), the g-factor can be expressed as

$$g(5s^2\,{}^1S_0) = \frac{2f_{\sigma^{\pm},m_F} - f_{d,m_F}}{2\mu_0 B}. \quad (11)$$

According to the measured values of $f_{\sigma^{\pm},m_F}$ and f_{d,m_F} in different magnetic field strengths, the value of $g(5s^2\,{}^1S_0)$ can also be obtained. The measured results are presented in Fig. 4(b). Therefore, the value of $g(5s^2\,{}^1S_0)$ is obtained to be $-1.306(52) \times 10^{-4}$ by linearly fitting of the experimental data.

In Table 1, we list the theoretical and experimental estimations of the ground state g-factor $g(5s^2\,{}^1S_0)$ and the differential g-factor between the $5s^2\,{}^1S_0$ state and the $5s5p\,{}^3P_0$ state for the ^{87}Sr atoms. It can be seen that our results of δg obtained from the π-transition spectra and the $\sigma^{\pm}$-transition spectra agree well with the measurement in Ref. [23]. The value of $g(5s^2\,{}^1S_0)$ measured in our experiment also matched well with the theoretical estimation in which the diamagnetic correction was taken into account. With the measured values of $g(5s^2\,{}^1S_0)$ and δg, the g-factor of the ${}^3P_0$ state is obtained, as listed in Table 1.

Table 1. Theoretical and experimental estimations of the Landé g-factor for the $5s^2\ ^1S_0$ state and the differential g-factor δg between the $5s^2\ ^1S_0$ state and the $5s5p\ ^3P_0$ state of the ^{87}Sr atom.

	Methods	$g(5s^2\ ^1S_0)$	δg	$g(5s5p\ ^3P_0)$
Theoretical	BW[23]		$-7.80(7)\times10^{-5}$	-2.097×10^{-4}
	MBW[23]		$-8.42(36)\times10^{-5}$	-2.159×10^{-4}
	Eff-core[32]		$-9.29(107)\times10^{-5}$	-2.246×10^{-4}
	Refs. [33,34]		-7.57×10^{-5}	
	Ref. [23]	-1.317×10^{-4}		
Experimental	$\sigma^{\pm}$-transition spectra[23]		$-7.75(29)\times10^{-5}$	-2.092×10^{-4}
	$\sigma^{\pm}$-transition spectra	$-1.306(52)\times10^{-4}$	$-7.72(43)\times10^{-5}$	-2.078×10^{-4}
	π-transition spectra		$-7.67(36)\times10^{-5}$	-2.073×10^{-4}

In summary, we have measured the g-factor of the ground state and the differential g-factor between the $5s^2\ ^1S_0$ state and the $5s5p\ ^3P_0$ state using the π-transition spectra and the $\sigma^{\pm}$-transition spectra in the ultra-cold ^{87}Sr atom system. In our measurement of the $\sigma^{\pm}$-transition spectra, the calibration of the external magnetic field is unnecessary. The ground state g-factor $g(5s^2\ ^1S_0)$ measured in our experiment agrees well with the previous theoretical prediction, and the consistence between our measured differential g-factor and the previous report is very good. Our measurements can quantitatively determine the Zeeman shift of the clock transition, which is helpful for improving the accuracy of the ^{87}Sr optical lattice clock. Moreover, this method can also be used for determining the differential g-factor of the clock states for the optical clocks based on other atoms.

References

[1] Poli N, Oates C W, Gill P and Tino G M 2013 *Riv. Nuovo Cimento* **36** 555
[2] Ludlow A D, Boyd M M, Ye J, Peik E and Schmidt P O 2015 *Rev. Mod. Phys.* **87** 637
[3] Takamoto M, Takano T and Katori H 1872 *Nature* **5** 288
[4] Akatsuka T, Takamoto M and Katori H 2010 *Phys. Rev.* A **81** 023402
[5] Weyers S, Lipphardt B and Schnatz H 2009 *Phys. Rev.* A **79** 031803
[6] Turyshev S G 2009 *From Quantum to Cosmos: Fundamental Physics Research in Space* (Singapore: World Scientific) chap 3 p 57
[7] Rosenb, T, Hume D B, Schmidt P O, Chou C W, Brusch A, Lorini L, Oskay W H, Drullinger R E, Fortier T M, Stalnaker J E, Diddams S A, Swann W C, Newbury N R, Itano W M, Winel, D J and Bergquist J C 2008 *Science* **319** 1808
[8] Norcia M A, Cline J R K and Thompson J K 2017 *Phys. Rev.* A **96** 042118
[9] Cairncross W B, Gresh D N, Grau M, Cossel K C, Roussy T S, Ni Y, Zhou Y, Ye J and Cornell E A 2017 *Phys. Rev. Lett.* **119** 153001
[10] Major F G 2007 *The Quantum Beat: Principles And Applications Of Atomic Clocks* (New York: Springer) vol 2 chap 19 p 417
[11] Grewal M S, Andrews A P and Bartone C G 2013 *Global Navigation Satellite Systems, Inertial Navigation And Integration* (New York: John Wiley & Sons) chap 2 p 9
[12] Gill P 2011 *Philos. Trans. R. Soc.* A **369** 4109
[13] B, Y B and Osherov I 2011 *Phys. Rev.* A **84** 013822
[14] Tscherbul T V, Brumer P and Buchachenko A A 2016 *Phys. Rev. Lett.* **117** 143201
[15] Bloom B J, Nicholson T L, Williams J R, Campbell S L, Bishof M, Zhang X, Zhang W, Bromley S L and Ye J 2015 *Nature* **506** 71
[16] Ichiro U, Masao T, Manoj D, Takuya O and Hidetoshi K 2015 *Nat. Photon.* **9** 185
[17] Lahaye B and Margerie J 1975 *J. Phys. France* **36** 943
[18] Porsev S G, Safronova U I and Safronova M S 2017 *Phys. Rev.* A **96** 012509
[19] Itano W M 2000 *J. Res. Natl. Inst. Stand. Technol.* **105** 829
[20] Tommaseo G, Pfeil T, Revalde G, Werth G, Indelicato P and Desclaux J P 2003 *Eur. Phys. J.* D **25** 113
[21] Meggers W F 1967 *J. Res. Natl. Bur. Stand.* **71A** 396
[22] Porsev S G, Derevianko A and Fortson E N 2004 *Phys. Rev.* A **69** 021403
[23] Boyd M M, Zelevinsky T, Ludlow A D, Blatt S, Zanon-Willette T, Foreman S M and Ye J 2007 *Phys. Rev.* A **76** 022510
[24] Rosenb, T, Schmidt P O, Hume D B, Itano W M, Fortier T M, Stalnaker J E, Kim K, Diddams S A, Koelemeij J C J, Bergquist J C and Wineland D J 2007 *Phys. Rev. Lett.* **98** 220801
[25] Xu Q, Liu H, Lu B, Wang Y, Yin M, Kong D, Ren J, Tian X and Chang H 2015 *Chin. Opt. Lett.* **13** 100201
[26] Ovsiannikov V D, Pal'chikov V G, Taichenachev A V, Yudin V I, Katori H and Takamoto M 2007 *Phys. Rev.* A **75** 020501
[27] Boyd M M, Ludlow A D, Blatt S, Foreman S M, Ido T, Zelevinsky T and Ye J 2007 *Phys. Rev. Lett.* **98** 083002
[28] Brusch A, Targat R L, Baillard X, Fouché M and Lemonde P 2006 *Phys. Rev. Lett.* **96** 103003
[29] Lemonde P 2009 *Eur. Phys. J. Spec. Top.* **172** 81
[30] Kopfermann H 1963 *Nuclear Moments* (New York: Academic Press)
[31] Olschewski L 1972 *Z. Phys.* **249** 205
[32] Santra R, Christ K V and Greene C H 2004 *Phys. Rev.* A **69** 042510
[33] Takamoto M, Hong F L, Higashi R, Fujii Y, Imae M and Katori H 2006 *J. Phys. Soc. Jpn.* **75** 104302
[34] Katori H, Takamoto M, Pal'chikov V G and Ovsiannikov V D 2003 *Phys. Rev. Lett.* **91** 173005